Journal of Power Sources 200 (2012) 77–82

Contents lists available at SciVerse ScienceDirect

Journal of Power Sources

journal homepage: www.elsevier.com/locate/jpowsour

A new direction for the performance improvement of rechargeable lithium/sulfur batteries

Sheng S. Zhang*, Jeffrey A. Read

U.S. Army Research Laboratory, RDRL-SED-C, Adelphi, MD 20783-1197, USA

ARTICLE INFO

Article history:
Received 26 September 2011
Received in revised form 17 October 2011
Accepted 19 October 2011
Available online 25 October 2011

Keywords:
Lithium/sulfur battery
Sulfur
Polysulfide
Catholyte
Lithium plating

ABSTRACT

In this work we introduce a new direction for the performance improvement of rechargeable lithium/sulfur batteries by employing an electrolyte that promotes Li anode passivation in lithium polysulfide solutions. To examine our concept, we assemble and characterize Li/Li_2S_9 liquid cells by using a porous carbon electrode as the current collector and a 0.25 m Li_2S_9 solution as the catholyte. Results show that Li/Li_2S_9 liquid cells are superior to conventional Li/S cells in specific capacity and capacity retention. We also find that use of $LiNO_3$ as a co-salt in the Li_2S_9 catholyte significantly increases the cell's Coulombic efficiency. More importantly, the cells with $LiNO_3$ have a ~2.5 V voltage plateau before the end of charging and demonstrate a steep voltage rise at the end of charging. The former is indicative of the formation of elemental sulfur from soluble lithium polysulfides on the carbon electrode, and the latter provides a distinct signal for full charging. Electrochemical analyses on Li plating and stripping in Li_2S_9 catholyte solutions indicate that $LiNO_3$ participates in the formation of a highly protective passivation film on the Li metal surface, which effectively prevents the Li anode from chemical reaction with polysulfide anions in the electrolyte and meanwhile prevents polysulfide anions from electrochemical reduction on the Li surface.

Published by Elsevier B.V.

1. Introduction

Lithium/sulfur (Li/S) batteries have attracted increasing interest in developing high density energy storage devices due to their high theoretical capacity. Based on the complete reduction of elemental sulfur to lithium sulfide (Li_2S), Li/S batteries can deliver a specific capacity as high as 1675 mAh g^{-1} sulfur. However, the specific capacity of a practical cell is lower than the theoretical value and the cell suffers low charging efficiency, high self-discharge and short cycle life [1,2]. All these problems are known to be related to the high solubility of lithium polysulfides, the series of sulfur reduction intermediates, in organic electrolyte solutions. Dissolution of lithium polysulfides not only results in the loss of sulfur active materials from the cathode, but also causes serious "redox shuttle" reactions between polysulfide anions in the electrolyte and the Li metal anode. Recently, a number of publications have reported a reduction in the dissolution of lithium polysulfides by making sulfur-carbon composite materials [3–14]. Based on physical adsorption, these composites in different contexts reduce the dissolution of lithium polysulfides from the cathode. However, these approaches are fundamentally ineffective since polysulfide anions carry negative charges, in discharging the electric field between two electrodes will drive polysulfide anions migrating toward Li anode. Furthermore, the incorporation of electrochemically inert carbons reduces the gravimetric energy density of Li/S batteries. In addition, we have noticed that most of decent capacities reported previously were obtained through two lows, that is, low sulfur content in composition and low sulfur loading in cathode. In many cases, the total sulfur content in the cathode is not more than 65% by weight and the sulfur loading is not higher than 2 mg sulfur per cm^2 of cathode [4–7,14–18].

Since dissolution of lithium polysulfides (Li_2S_x, $x > 2$) in organic electrolytes is inevitable, in this work we propose a different approach for the performance improvement of rechargeable Li/S batteries by employing a liquid electrolyte that is able to promote the formation of a highly protective passivation film on lithium surface in lithium polysuiifide solutions. We expect that the resulting passivation film not only protects lithium metal from chemical reaction with the polysulfide anions but also prevents polysulfide anions from electrochemical reduction on the Li anode. Our effort will be focused on increasing Li cycling efficiency in highly concentrated lithium polysulfide solutions. To examine our idea, we selected Li/Li_2S_9 liquid cell [19,20], instead of the conventional Li/S cell, as the testing vehicle by employing a porous carbon electrode as the cathode current collector and a Li_2S_9 solution as the catholyte. Due to the known ability of $LiNO_3$ in facilitating the formation of a better passivation film on Li metal surface [21,22], in this work we study the effect of $LiNO_3$ on cycling performance

* Corresponding author. Tel.: +1 301 394 0981; fax: +1 301 394 0273.
E-mail address: shengshui.zhang@us.army.mil (S.S. Zhang).

0378-7753/$ – see front matter. Published by Elsevier B.V.
doi:10.1016/j.jpowsour.2011.10.076

of Li/Li_2S_9 liquid cells and on cycling efficiency of Li metal in Li_2S_9 catholyte solutions by adding $LiNO_3$ as a co-salt of the Li_2S_9 catholyte.

2. Experimental

Elemental sulfur (S_8, 99.5%), lithium sulfide (Li_2S, 99%), and lithium nitrate ($LiNO_3$, 99.99%) were purchased from Aldrich and used as received. Lithium bis(trifluoromethane sulfone)imide ($LiN(SO_2CF_3)_2$, LiTFSI, 3M Company) was dried at 110 °C under vacuum for 10 h and triethylene glycol dimethyl ether (TG3, 99%, Aldrich) was dried over 4 Å molecular sieves for a week. For conventional Li/S cells, a liquid electrolyte was prepared by dissolving 0.2 m (molality) LiTFSI in TG3 in Ar-filled glove-box and a sulfur cathode with a composition of 77% S, 20% Super-P carbon and 3% binder by weight was coated onto a carbon-coated aluminum foil by using poly(acrylonitrile-methyl methacrylate) (ANMMA, AN/MMA = 94:6, MW = 100 000, Polysciences Inc.) as binder and N-methyl pyrrolidinone (NMP) as solvent. Resulting cathode, dried at 80 °C under vacuum for 2 h, had an average loading of 2.4 mg sulfur per cm^2. For Li/Li_2S_9 liquid cells, a carbon electrode having a composition of 90% Super-P carbon and 10% binder by weight was prepared using the same materials and procedure as was used in preparation of the sulfur cathode and dried at 110 °C under vacuum for 10 h. The carbon electrode was measured to have an average loading of 0.78 mg carbon per cm^2.

Following Rauh et al's procedure [19,23], lithium polysulfide (Li_2S_x, $x = 9$) solution was prepared by adding stoichiometric amounts of elemental sulfur (S_8) and Li_2S into the electrolyte solution, followed by heating at 80 °C with magnetic stirring for 6 h. In this work, we prepared two catholyte solutions with composition below:

Catholyte-A: 0.25 m Li_2S_9–0.2 m LiTFSI in TG3
Catholyte-B: 0.25 m Li_2S_9–0.1 m LiTFSI–0.2 m $LiNO_3$ in TG3

Both solutions were red-dark color and had moderate viscosity. Li/S coin cells with an electrode area of 1.27 cm^2 were assembled using sulfur cathode and filled with 10 μL electrolyte. Li/Li_2S_9 liquid cells were assembled by using a 1.27 cm^2 carbon electrode as the cathode current collector (also serving as catalyst for the reduction of elemental sulfur and lithium polysulfides) and 10 μL catholyte solution as the electrolyte and cathode. It should be noted that the assembly of Li/Li_2S_9 liquid cells should be conducted in an oxygen-free environment so as to avoid the oxidization of polysulfide anions by oxygen. For easy comparison with conventional Li/S cells, the specific capacity of Li/Li_2S_9 liquid cells was normalized as "mAh g^{-1} sulfur". Thus, the theoretical capacity of Li_2S_9 was calculated to be 1489 mAh g^{-1} sulfur (i.e., $1675 \times 8/9 = 1489$), and each Li/Li_2S_9 liquid cell contained ~1.65 mg sulfur as calculated based on the amount of Li_2S_9 in the catholyte.

Both Li/S and Li/Li_2S_9 cells were cycled at 0.2 mA cm^{-2} on a Maccor Series 4000 cycler with a 1.5 V discharge cutoff voltage. The charging process was terminated either by a 3.0 V cutoff voltage or by a capacity equaling to 150% of the last discharge capacity, whichever came first. To measure Li plating and stripping efficiency, a Li/Ni cell with a 1.27 cm^2 electrode area was assembled and cycled by discharging (Li plating) at 0.2 mA cm^{-2} for 1 h and then charging (Li stripping) until the cell's voltage reached 1.0 V. Coulombic efficiency of Li cycling was defined as the percentage of charging time over discharging time. In addition, three-electrode coin cells were assembled for electrochemical measurements by using a 0.97 cm^{-2} Ni foil as working electrode, two Li foils as the counter electrode and reference electrode, respectively. Detailed descriptions about cell structure and assembly procedure are referred to our previous works [24,25]. The impedance and cyclic voltammetry measurements were run on a Solartron SI 1287 Electrochemical Interface and a SI 1260 Impedance/Gain-Phase Analyzer. Impedance was measured at open-circuit potential (OCP) in the frequency range from 0.01 to 100 kHz with an ac oscillation of 10 mV amplitude. Before each test, the cell rested for 1 h after Li plating or Li stripping to get the same conditions.

3. Results and discussion

3.1. Li/S cell vs. Li/Li_2S_9 liquid cell

Fig. 1 shows voltage profiles of the first and fifth cycles of a conventional Li/S cell and a Li/Li_2S_9 liquid cell, respectively. For the conventional Li/S cell (Fig. 1a), the initial discharging consists of three voltage regions: (1) a short plateau at 2.3 V as indicated by the arrow, (2) a linear sloping decline, and (3) a long plateau at ~2.0 V until the end of discharge. Combining the conclusions of previous publications [16,26–29], we ascribe these three discharging voltage regions to the following three reactions:

$$S_8(\text{insoluble}) + 2Li \rightarrow Li_2S_8(\text{soluble}) \quad (1)$$

$$Li_2S_8(\text{soluble}) + 6Li \rightarrow 4Li_2S_2(\text{insoluble}) \quad (2)$$

$$Li_2S_2(\text{insoluble}) + 2Li \rightarrow 2Li_2S(\text{insoluble}) \quad (3)$$

In the following charge step, the cell voltage responds to the reversible processes of Eqs. (2) and (3) until 2.5 V, at which the voltage stays constantly, indicating that Eq. (1) is irreversible. In the fifth cycle, the voltage plateau observed at 2.3 V in the first cycle no longer appears, and the charge voltage does not exceed 2.5 V. For the Li/Li_2S_9 liquid cell (Fig. 1b), the first discharge does not show voltage plateau near 2.3 V since no elemental sulfur exists in the system. However, in the following charge, the cell voltage reaches 3.0 V, achieving a cycling efficiency of 91%. Discharging and charging voltage profiles of the fifth cycle are very similar as those observed in the conventional Li/S cell. We tested many other Li/Li_2S_9 cells and the similar results were repeatedly observed. It should be mentioned that except for the initial few cycles, both the Li/S and Li/Li_2S_9 cells cannot be charged to higher than 2.5 V, i.e., the reversal process of Eq. (1) does not occur. The reason is because soluble lithium polysulfides (Li_2S_x, $x > 2$), especially those having long S–S chain, dissolve and diffuse to the surface of the Li anode, where polysulfide anions not only are electrochemically reduced as described by Eq. (4) but also are chemically reacted with Li metal as described by Eq. (5).

$$(x-y)Li_2S_x + 2yLi^+ + 2ye^- \rightarrow xLi_2S_{x-y} \quad (4)$$

$$(x-y)Li_2S_x + 2yLi \rightarrow xLi_2S_{x-y} \quad (5)$$

Thus, the soluble polysulfide anions act as a redox shuttle between the cathode and Li anode, resulting in low charging efficiency.

Fig. 2 compares capacity retention of the conventional Li/S cell and Li/Li_2S_9 liquid cell. It is shown that these two cells have the similar initial capacities (about 610 mAh g^{-1} S) in spite of the fact that Li_2S_9 has a relatively lower theoretical capacity than elemental sulfur. However, the Li/Li_2S_9 cell exhibits more stable capacity retention. By the end of testing (50 cycles), the Li/Li_2S_9 cell remains 452 mAh g^{-1} capacity (equaling to 72% of the initial capacity), while the Li/S cell retains only 196 mAh g^{-1} S (32% of its initial capacity). These results reveal that Li/Li_2S_9 liquid cells are superior to the conventional Li/S cells in capacity retention.

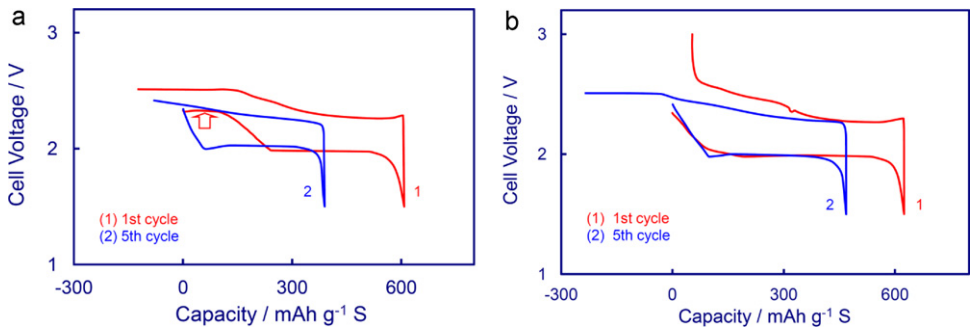

Fig. 1. Discharging voltage profiles of the first and fifth cycles of (a) a conventional Li/S cell and (b) a Li/Li_2S_9 liquid cell.

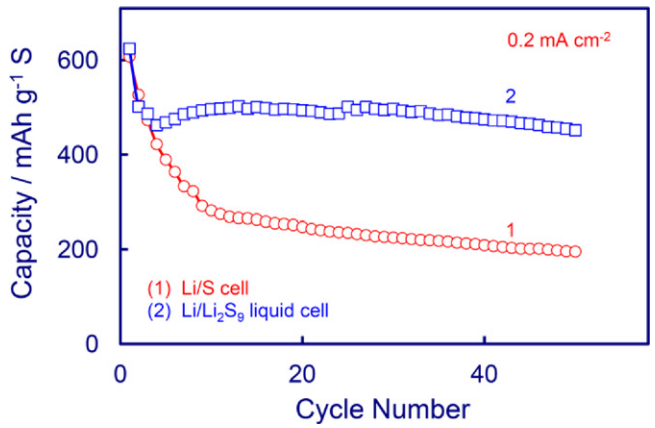

Fig. 2. Comparison of the capacity retention of a conventional Li/S cell and a Li/Li_2S_9 liquid cell.

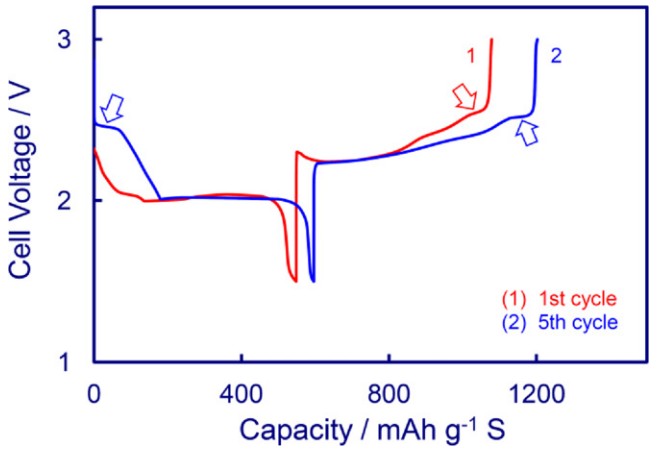

Fig. 4. Voltage profiles of the first and fifth cycles of a Li/Li_2S_9 liquid cell with Catholyte-B.

3.2. *Effect of $LiNO_3$ on cycling performance*

Reactions (4) and (5) are believed to be the main cause for the low charging efficiency and high self-discharge rate of Li/S batteries. Furthermore, their reaction products will permanently deposit on the surface of the Li anode if insoluble Li_2S_x ($x \leq 2$) is formed. When this happens, the performance of Li/S cells will be dramatically affected. For this reason, in this work we focused our effort on suppressing Reactions (4) and (5) by adding $LiNO_3$ as a co-salt in the Li_2S_9 catholyte. Fig. 3 compares discharging and charging voltage profiles of two Li/Li_2S_9 cells with and without $LiNO_3$ as co-salt. As indicated in Fig. 3a, the most significant difference between these two cells is that Cell-2 with $LiNO_3$-containing Catholyte-B can repeatedly be charged to 3 V while Cell-1 with Catholyte-A free of $LiNO_3$ can be charged above 2.5 V only in the first cycle. Another difference is that Cell-2 exhibits a pair of additional voltage plateaus at ~2.3 V in discharge and charge processes, as indicated by two arrows in Fig. 3b. This pair of voltage plateaus can be attributed to the reversible reaction of Eq. (1).

To further verify this, we plot discharge and charge curves for the first and fifth cycles of Cell-2 in Fig. 4. It can be seen that the first discharge does not show voltage plateau near 2.3 V although Li_2S_9 has a longer S–S chain than elemental sulfur (S_9 vs. S_8), instead, the fifth discharge shows a distinct plateau at 2.3 V. In charging, both the first and fifth cycles distinctly show a 2.3 V plateau, followed by a steep voltage rise to the cutoff voltage (3.0 V). These results indicate that the 2.3 V plateau is not related to the length of polysulfide anions (i.e., the x value in Li_2S_x), instead to the two-phase Reaction-1 occurring between Li_2S_x in solution and elemental sulfur in cathode.

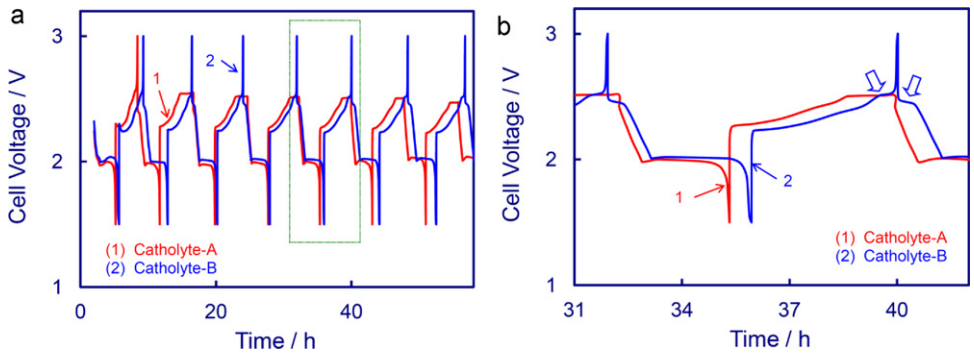

Fig. 3. Voltage profiles of the discharging and charging cycles of two Li/Li_2S_9 liquid cells with Catholyte-A and Catholyte-B, respectively: (a) overall view of the voltage profiles and (b) cell voltages of a typical cycle.

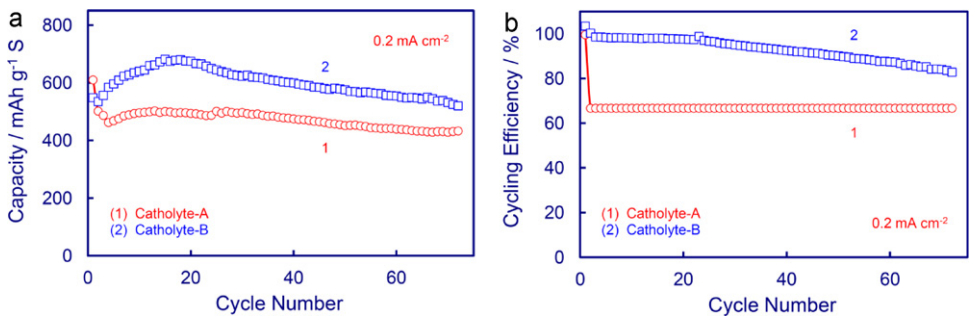

Fig. 5. Effect of $LiNO_3$ co-salt on cycling performance of Li/Li_2S_9 liquid cells: (a) capacity retention and (b) Coulombic efficiency of cycling.

The effect of $LiNO_3$ on cycling efficiency and capacity retention is presented in Fig. 5a and b, respectively, where Cell-1 uses Catholyte-A free of $LiNO_3$ and Cell-2 employs Catholyte-B containing 0.2 m $LiNO_3$. As compared with Cell-1, Cell-2 not only has higher capacity (Fig. 5a), but also has significantly higher Coulombic efficiencies (Fig. 5b). The latter would be the most important benefit added by the use of $LiNO_3$ co-salt. For Cell-1, except for the first cycle the charging voltages can never reach the cutoff voltage (3.0 V, see Fig. 3), all charging processes are ended by the pre-set charging time. Since we setup 150% of the last discharge capacity as one of the charge limits, Coulombic efficiencies for all cycles are 66.7% (i.e., the reciprocal of 150%). For Cell-2, charge voltages repeatedly reach the pre-set cutoff voltage and the charge processes are terminated by the cutoff voltage, resulting in higher Coulombic efficiencies.

3.3. *Understanding the role of $LiNO_3$ in Li/S cell*

Assuming that Reactions (4) and (5) are the main reason for low Coulombic efficiency of Li/S cells and that both reactions occur on the Li anode surface, we believe that the important role of $LiNO_3$ in Li/S cells can be understood from the viewpoint of the Li anode. Therefore, we place our attention on the plating and stripping behavior of Li metal in highly concentrated Li_2S_x ($x > 2$) solutions. Fig. 6 exhibits the potential curves of the first plating and stripping of Li metal on a fresh Ni surface in Catholyte-A and Catholyte-B, respectively. In Catholyte-A, the potential of Ni working electrode shows multiple plateaus between OCP and 1.3 V, followed by a slow and smooth decline. Even at the end of the plating test, the potential of Ni still remains at +0.15 V vs. Li/Li^+. This is because the Li metal plated on the Ni surface is not dense, measured is a mixed potential of the Li metal and polysulfide solution. Subsequent Li stripping test gives a 26% Li cycling efficiency. In Catholyte-B, the potential remains a plateau for 82 min, and then steeply drops to a constant negative value (−50 mV vs. Li/Li^+), at which Li plates progressively, giving a 50% cycling efficiency as shown by the subsequent Li stripping test. It is clearly shown that in both catholyte solutions, Li metal cannot be plated until a protective passivation film is formed on the Ni surface, and that such a film must be formed by the irreversible electrochemical reduction of polysulfides, as expressed by Eq. (4).

Coulombic efficiencies of Li plating and stripping in Catholyte-A and Catholyte-B are compared in Fig. 7. Obviously, the efficiencies in Catholyte-B are significantly higher than those obtained in Catholyte-A, verifying that $LiNO_3$ promotes the formation of a more protective (normally denser) passivation film. It is interesting to note that in both Cathode-A and Cathode-B, Li cycling efficiencies are increased slowly with cycle number, probably because the passivation film becomes denser and denser, resulting in better protection of Li metal from Reactions (4) and (5).

On the other hand, the essential role of $LiNO_3$ in the formation of a passivation film on the Li surface can be examined by impedance analyses. Fig. 8 shows the impedance spectrums of the Ni surface after Li plating and after subsequent Li stripping. For the Li-plated Ni surfaces indicated by Curves 1 and 2 in Fig. 8, the impedance spectrum is composed of two flatted semicircles. In general, the semicircle in higher frequency range corresponds to a passivation film and the one in lower frequency range corresponds to the charge-transfer process occurring on the electrolyte–electrode interface [30,31]. For Li metal electrode, the charge-transfer usually reflects the following reversible electrochemical process:

$$Li - e^- \Leftrightarrow Li^+ \quad (6)$$

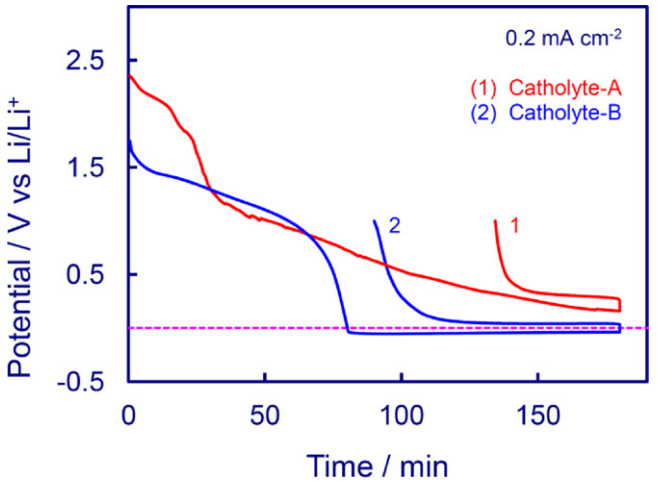

Fig. 6. Potential profiles of the first Li plating and stripping on a fresh Ni surface, which were recorded at 0.2 mA cm^{-2} for 3 h on a 3-electrode cell: (1) Catholyte-A and (2) Catholyte-B.

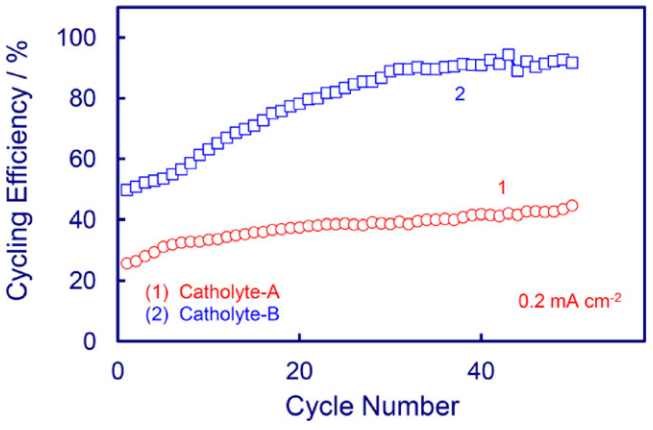

Fig. 7. Coulombic efficiency of Li plating and stripping on Ni surface in Catholyte-A and Catholyte-B, respectively.

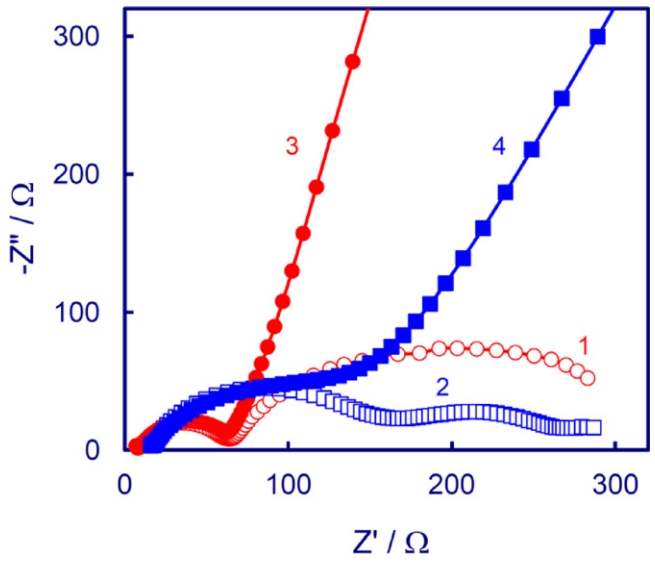

Fig. 8. Impedance spectroscopes of a Ni electrode in Catholyte-A and Catholyte-B, respectively, which were recorded at open-circuit potential on a 3-electrode cell: (1) after Li plating at 0.2 mA cm^{-2} for 3 h in Catholyte-A, (2) after Li plating at 0.2 mA cm^{-2} for 3 h in Catholyte-B, (3) after Li stripping at 0.2 mA cm^{-2} to 1.0 V following (1), and (4) after Li stripping at 0.2 mA cm^{-2} to 1.0 V following (2).

Comparison of Curves 1 and 2 shows that the Li metal plated in Catholyte-B (Curve-2) has a higher passivation resistance and a much lower charge-transfer resistance. The higher passivation resistance is a good indication that the passivation film formed in the presence of $LiNO_3$ co-salt is denser and hence more protective. After subsequent Li stripping, the charge-transfer process as expressed by Eq. (6) no longer takes place due to the absence of Li metal, and therefore the semicircle in the lower frequency range disappears as indicated by Curves 3 and 4, respectively. By comparing Curve-1 with Curve-3 and Curve-2 with Curve-4, one sees that the passivation film still remains even after Li stripping, indicating that the passivation film is permanently present on the electrode surface once it has formed.

The benefit of $LiNO_3$ also can be observed from cyclic voltammetric results as shown in Fig. 9. First, the cyclic voltammogram (CV) in Catholyte-B has much higher peak currents. This result coincides with the impedance results (i.e., much lower charge-transfer resistance in Catholyte-B). Second, the CV in Catholyte-B gives much higher Li cycling efficiency (i.e., 65% vs. 29% in Catholyte-A, calculated from the cyclic voltammograms). This result agrees with those obtained from galvanostatic plating and stripping tests as shown in Fig. 7. Third, Li platting in Catholyte-B has no polarization while that in Catholyte-A shows polarization, as indicated by the arrow in Fig. 9.

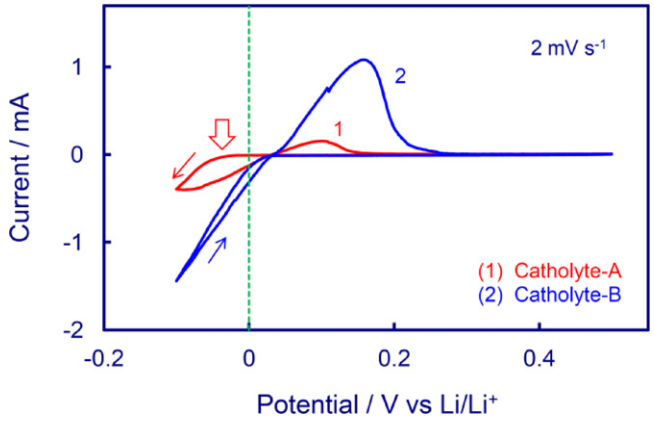

Fig. 9. Cyclic voltammograms of Ni electrode in Catholyte-A and Catholyte-B, which were recorded by scanning potential at 2 mV s^{-1} between 0.1 V and 0.5 V vs. Li/Li$^+$.

Based on the discussion above, the charging voltage profiles of Cell-2 in Figs. 3a, b and 4 can be explained as follows: as Eq. (5) shows, Li metal and Li_2S_x chemically react with each other. While protecting Li metal, the passivation film meanwhile protects Li_2S_x from attack by the highly reductive Li metal. Moreover, the passivation film serves as a solid electrolyte interphase (SEI) to prevent soluble Li_2S_x ($x > 2$), especially those species having long S–S chain near the full charge state, from being electrochemically reduced, as expressed by Eq. (4). Instead, the soluble Li_2S_x species are electrochemically oxidized to elemental sulfur on the cathode, resulting in an additional voltage plateau at 2.3 V, higher charging efficiency, and accordingly a steep voltage rise upon the full charge.

4. Conclusions

This work demonstrates an alternative approach for the performance improvement of rechargeable Li/S batteries. While dissolution of lithium polysulfides (Li_2S_x, $x > 2$) in organic electrolytes is inevitable, research efforts focusing on the protection of the lithium anode to increase Li cycling efficiency in highly concentrated polysulfide solutions may be more feasible. $LiNO_3$ is excellent in promoting the formation of a denser and more protective passivation film on the Li surface. The film formed not only increases Li cycling efficiency, but also protects soluble polysulfide anions from chemical and electrochemical reductions on the Li anode. Use of $LiNO_3$ as a co-salt makes the two-phase reaction of "S_8 (insoluble) + 2Li → Li_2S_8 (soluble)" reversible, resulting in a 2.3 V plateau, higher specific capacity and higher charging efficiency. Moreover, Li/S cells with $LiNO_3$ co-salt can be repeatedly charged to cutoff voltage (>2.5 V) and indicate a steep voltage rise as the signal of full charge. On the contrary, the conventional Li/S cells can only be charged to 2.5 V at which the voltage stays constant until the charging process is manually terminated, resulting in low specific capacity and low charging efficiency, due to the chemical and electrochemical reductions of polysulfide anions on the Li anode.

References

[1] Y.V. Mikhaylik, J.R. Akridge, J. Electrochem. Soc. 151 (2004) A1969.
[2] V.S. Kolosnitsyn, E.V. Karaseva, Russ. J. Electrochem. 44 (2008) 506.
[3] J.L. Wang, J. Yang, J.Y. Xie, N.X. Xu, Y. Li, Electrochem. Commun. 4 (2002) 499.
[4] Y.J. Choi, Y.D. Chung, C.Y. Baek, K.W. Kim, H.J. Ahn, J.H. Ahn, J. Power Sources 184 (2008) 548.
[5] C. Lai, X.P. Gao, B. Zhang, T.Y. Yan, Z. Zhou, J. Phys. Chem. C 113 (2009) 4712.
[6] X. Ji, K.T. Lee, L.F. Nazar, Nat. Mater. 8 (2009) 500.
[7] C. Liang, N.J. Dudney, J.Y. Howe, Chem. Mater. 21 (2009) 4724.
[8] B. Zhang, C. Lai, Z. Zhou, X.P. Gao, Electrochim. Acta 54 (2009) 3708.
[9] L. Yuan, H. Yuan, X. Qiu, L. Chen, W. Zhu, J. Power Sources 189 (2009) 1141.
[10] C. Wang, J.j. Chen, Y.N. Shi, M.S. Zheng, Q.F. Dong, Electrochim. Acta 55 (2010) 7010.
[11] B. Zhang, X. Qin, G.R. Li, X.P. Gao, Energy Environ. Sci. 2 (2010) 1531.
[12] J.Z. Wang, L. Lu, M. Choucair, J.A. Stride, X. Xu, H.K. Liu, J. Power Sources 196 (2011) 7030.
[13] H. Wang, Y. Yang, Y. Liang, J.T. Robinson, Y. Li, A. Jackson, Y. Cui, H. Dai, Nano Lett. 11 (2011) 2644.
[14] S.R. Chen, Y.P. Zhai, G.L. Xu, Y.X. Jiang, D.Y. Zhao, J.T. Li, L. Huang, S.G. Sun, Electrochim. Acta (2011), doi:10.1016/j.electacta.2011.03.005.
[15] S.E. Cheon, K.S. Ko, J.H. Cho, S.W. Kim, E.Y. Chin, H.T. Kim, J. Electrochem. Soc. 150 (2003) A800.
[16] H.S. Ryu, H.J. Ahn, K.W. Kim, J.H. Ahn, J.Y. Lee, J. Power Sources 153 (2006) 360.
[17] Y.J. Choi, K.W. Kim, H.J. Ahn, J.H. Ahn, J. Alloys Compd. 449 (2008) 313.
[18] J.J. Chen, X. Jia, Q.J. She, C. Wang, Q. Zhang, M.S. Zheng, Q.F. Dong, Electrochim. Acta 55 (2010) 8062.
[19] R.D. Rauh, K.M. Abraham, G.F. Pearson, J.K. Surprenant, S.B. Brummer, J. Electrochem. Soc. 126 (1979) 523.
[20] H. Yamin, A. Gorenshtein, J. Penciner, Y. Sternberg, E. Peled, J. Electrochem. Soc. 135 (1988) 1045.

[21] Y.V. Mikhaylik, U.S. Patent (2008) 7,352,680.
[22] D. Aurbach, E. Pollak, R. Elazari, G. Salitra, C.S. Kelley, J. Affinito, J. Electrochem. Soc. 156 (2009) A694.
[23] R.D. Rauh, F.S. Shuker, J.M. Marston, S.B. Brummer, J. Inorg. Nuclear Chem. 39 (1977) 1761.
[24] S.S. Zhang, J. Power Sources 163 (2006) 567.
[25] S.S. Zhang, J. Power Sources 163 (2007) 713.
[26] S.E. Cheon, K.S. Ko, J.H. Cho, S.W. Kim, E.Y. Chin, H.T. Kim, J. Electrochem. Soc. 150 (2003) A796.
[27] J.R. Akridge, Y.V. Mikhaylik, N. White, Solid State Ionics 175 (2004) 243.
[28] S.S. Jeong, Y.T. Lim, Y.J. Choi, G.B. Cho, K.W. Kim, H.J. Ahn, K.K. Cho, J. Power Sources 174 (2007) 745.
[29] H.S. Ryu, Z. Guo, H.J. Ahn, G.B. Cho, H. Liu, J. Power Sources 189 (2009) 1179.
[30] S.S. Zhang, M.H. Ervin, D.L. Foster, K. Xu, T.R. Jow, J. Solid State Electrochem. 9 (2005) 77.
[31] S.S. Zhang, J. Power Sources 180 (2008) 586.